

Coaligned Dual-Channel STED Nanoscopy and Molecular Diffusion Analysis at 20 nm Resolution

Fabian Göttfert,[†][△] Christian A. Wurm,[†][△] Veronika Mueller,[†] Sebastian Berning,[†] Volker C. Cordes,[‡] Alf Honigmann,[†] and Stefan W. Hell^{†*}

[†]Department of NanoBiophotonics and [‡]Department of Cellular Logistics, Max Planck Institute for Biophysical Chemistry, Göttingen, Germany

ABSTRACT We report on a fiber laser-based stimulated emission-depletion microscope providing down to ~20 nm resolution in raw data images as well as 15–19 nm diameter probing areas in fluorescence correlation spectroscopy. Stimulated emission depletion pulses of nanosecond duration and 775 nm wavelength are used to silence two fluorophores simultaneously, ensuring offset-free colocalization analysis. The versatility of this superresolution method is exemplified by revealing the octameric arrangement of *Xenopus* nuclear pore complexes and by quantifying the diffusion of labeled lipid molecules in artificial and living cell membranes.

Received for publication 29 March 2013 and in final form 17 May 2013.

[△]Fabian Göttfert and Christian A. Wurm contributed equally to this work.

*Correspondence: shell@gwdg.de

This is an Open Access article distributed under the terms of the Creative Commons-Attribution Noncommercial License (<http://creativecommons.org/licenses/by-nc/2.0/>), which permits unrestricted noncommercial use, distribution, and reproduction in any medium, provided the original work is properly cited.

Since its first demonstration in (live) cell imaging (1), stimulated emission depletion (STED) fluorescence microscopy has been realized in many variants. Particularly, the key phenomenon employed in this method, namely switching fluorophores transiently off by stimulated emission, has been accomplished with laser pulses varying from picoseconds to nanoseconds in duration, and from kHz to MHz in repetition rate. Because continuous-wave beams are suitable as well (2), STED microscopy has been implemented with rather different laser systems, ranging from modelocked femtosecond to continuous-wave laser diodes (3,4). Although it underscores the versatility of STED to modulate the fluorescence capability of a fluorophore, this wide range of options may confuse adopters when balancing simplicity, applicability, and resolution gain. The situation is exacerbated when implementing pairs of excitation and STED beams for dual-color colocalization studies (5,6).

Here we report on a simple arrangement providing dual-color STED nanoscopy (Fig. 1) and molecular diffusion quantification down to ~20 nm in (living) cells. The presented dual-channel STED microscope utilizes a single fiber laser providing a 20-MHz train of 775 nm wavelength pulses of 1.2-ns duration. This compact laser source enables STED on fluorophores emitting in the orange to red range. Specifically, we applied this laser on the orange dyes Atto590 and Atto594 (excitation: 595 nm; detection: 620 ± 20 nm), and the red dyes KK114 and Abberior Star635P (excitation: 640 nm; detection: 670 ± 20 nm). Although the spectra of the dyes are partially overlapping, the individual color channels can be separated without data

processing (see Fig. S1 and Fig. S2 in the Supporting Material). Both channels are recorded simultaneously within 50 ns, using temporally interleaved pulsed excitation in combination with time-gated detection (5,7,8).

Because in STED microscopy, the STED doughnuts firmly determine the position of the fluorescently active molecules, the use of a single doughnut for both fluorophores guarantees that the two color channels are almost perfectly coaligned. The use of the doughnut even counteracts misalignments of the confocal excitation and detection channels (Fig. 2, and see Fig. S3), making STED microscopy particularly powerful for colocalization measurements.

The cross section for stimulated emission is lower at 775 nm as compared to that found at somewhat shorter wavelengths (5), yet STED pulse energies of ~7 nJ in the focus are sufficient to yield a resolution of ~30 nm and ~20 nm in the orange and red channels, respectively (see Fig. S4). In addition, due to the lower peak intensity, the 1.2 ns pulses are likely to induce less nonlinear absorption and hence less photostress as compared to their more commonly used <0.2 ns counterparts (8,9). On the other hand, the pulses are only 2–4 times shorter than the typical lifetime of the excited state, which lessens their STED efficiency. This slight reduction is neutralized here by detecting photons emitted ~1 ns after excitation (5,7,8).

Editor: Paul Wiseman.

© 2013 by the Biophysical Society

<http://dx.doi.org/10.1016/j.bpj.2013.05.029>



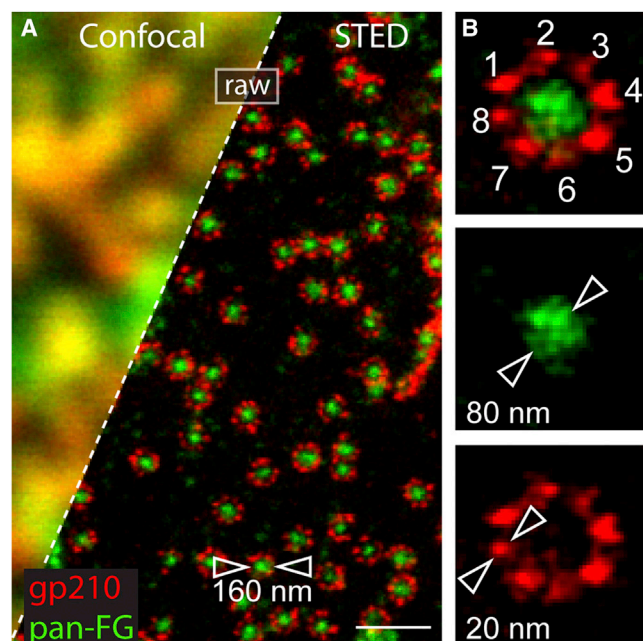


FIGURE 1 Fluorescence nanoscopy of protein complexes with a compact near-infrared nanosecond-pulsed STED microscope. (A) STED reveals immunolabeled subunits in amphibian NPC; raw data smoothed with a Gaussian filter extending over 14 nm in FWHM. The diameter of the octameric gp210 ring is established as ~160 nm. Scale bar, 500 nm. (B) Individual NPC image showing eight antibody-labeled gp210 homodimers as 20–40 nm sized units and a 80 nm-sized localization of the subunits in the central channel.

The potential of this straightforward implementation of STED microscopy is evident when imaging immunolabeled nuclear pore complexes (NPCs) of cultured *Xenopus* cells. Contrary to the confocal recording, STED microscopy reveals subunits of this protein complex, specifically the typical eightfold symmetry of its peripheral transmembrane protein gp210, along with a set of proteins in the central pore channel (Fig. 1, and see Fig. S5 and Fig. S6). Unlike in stochastic superresolution imaging of gp210 (10), the color channels are inherently coaligned and simultaneously recorded simply by executing a single scan. Apart from a weak smoothing and background subtraction applied to enhance image contrast, the images are raw.

Because fluorescence off-switching by STED is an instant process, STED microscopy can be employed to study fast spatial translocations, such as the diffusion of molecules on the nanoscale (3). To benchmark the performance of our setup, we analyzed the diffusion of a fluorescent glycerophospholipid analog (11) by fluorescence correlation spectroscopy (FCS) in membranes of living mammalian PtK2-cells (Fig. 3). STED allowed us to reduce the diameter of the probed area from the 250 nm-sized diffraction limit down to 19 nm (FWHM), representing $\sigma = 8$ nm in standard deviation of a Gaussian

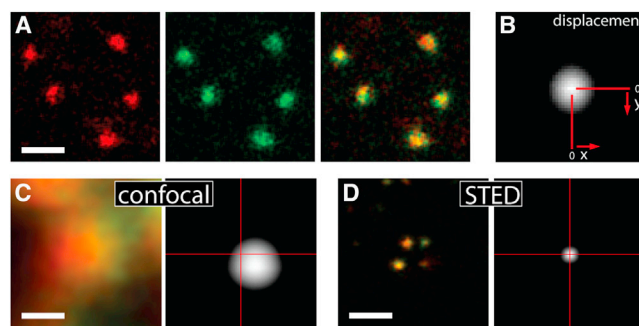


FIGURE 2 Determination of the colocalization accuracy. *Xenopus* A6 cells, labeled with an antiserum against multiple NUP subunits in the central NPC channel and two secondary antibodies decorated with the fluorophores Abberior STAR635P and Atto594 were imaged by STED microscopy. (A) Upon overlaying both channels, a high degree of colocalization is directly visible. Scale bar, 200 nm. (B) Quantification of the colocalization by cross correlation of much larger images (see Fig. S3). The correlation is maximal for zero displacement of the images, proving colocalization. (C) Confocal image of monocolored fluorescent beads taken with improperly coaligned excitation beams (left). Improper coalignment spoils the colocalization accuracy in confocal imaging; the two channels should be perfectly coaligned, but they show a false offset as indicated by the color difference. The offset is quantified by the cross correlation of the two channels (right). (D) The STED image of the same beads (left) not only shows 10-fold improved resolution over the confocal image in panel C, but also improved colocalization, again quantified by cross correlation (right). Thus, by predetermining the position of emission, the STED doughnut counteracts errors induced by imperfect coalignment of the two confocal color channels (for details, see Fig. S3). Scale bars = 100 nm.

fit. The attained subdiffraction area is 2.5 times smaller as compared to what has been reported in living cells to date (4). In model membranes, the smallest diameter was 15 nm ($\sigma = 6.4$ nm).

In both measurements, the molecular transit time depends linearly on the probed area, indicating that the labeled lipid molecules diffuse essentially freely down to spatial scales of 20 nm. Accordingly, the anomaly exponent α was close to 1 with values of $\alpha > 0.85$, showing only minor deviations from free diffusion (see Fig. S7). Because the diameter is inversely proportional to the square-root of the STED beam power, the resolution can be adapted to a particular application need (Fig. 3, A and B).

In summary, our arrangement provides up-to-date STED microscopy resolution in offset-free colocalization recordings. The ready-to-use near-infrared laser pulses keep undesired single and multiphoton absorption low and leave the visible spectrum amenable for further studies.

SUPPORTING MATERIAL

Seven figures, methods and materials, and references (12–17) are available at [http://www.biophysj.org/biophysj/supplemental/S0006-3495\(13\)00612-7](http://www.biophysj.org/biophysj/supplemental/S0006-3495(13)00612-7).

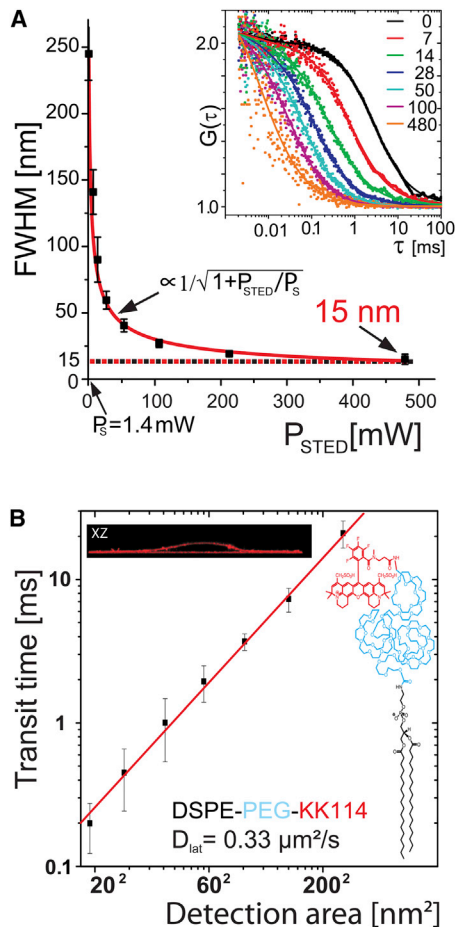


FIGURE 3 Nanoscale molecular diffusion analyzed by STED FCS. (A) For moderate and larger STED beam power P_{STED} , the resolution scales inversely with its square-root, attaining 15 nm in FWHM of the distribution of fluorescence emission in space, describing the measurement area. Note the relatively small threshold power $P_S = 1.4$ mW, which implies that a large resolution gain is already attained for $P_{\text{STED}} < 100$ mW. (Inset) The resolution was determined by measuring the transit time of a fluorescent phospholipid-analog (DSPE-PEG-KK114) in a lipid model membrane through the detection area by FCS. (B) In living mammalian Ptk2-cells, the transit time of the lipid analog scales linearly with the detection area, revealing a diffusion constant $D_{\text{lat}} = 0.33 \mu\text{m}^2/\text{s}$, and showing that this lipid analog diffuses largely freely in the plasma membrane down to < 20 nm scales.

ACKNOWLEDGMENTS

We thank E. Rothermel and T. Gilat for technical assistance, A. Schönle for the software ImSpector, and J. Jethwa for critical reading.

S.W.H. acknowledges support by the Körber Foundation.

REFERENCES and FOOTNOTES

1. Klar, T. A., S. Jakobs, ..., S. W. Hell. 2000. Fluorescence microscopy with diffraction resolution barrier broken by stimulated emission. *Proc. Natl. Acad. Sci. USA*. 97:8206–8210.
2. Vicidomini, G., G. Moneron, ..., S. W. Hell. 2011. Sharper low-power STED nanoscopy by time gating. *Nat. Methods*. 8:571–573.
3. Schrof, S., T. Staudt, ..., S. W. Hell. 2011. STED nanoscopy with mass-produced laser diodes. *Opt. Express*. 19:8066–8072.
4. Eggeling, C., C. Ringemann, ..., S. W. Hell. 2009. Direct observation of the nanoscale dynamics of membrane lipids in a living cell. *Nature*. 457:1159–1162.
5. Bückers, J., D. Wildanger, ..., S. W. Hell. 2011. Simultaneous multi-lifetime multi-color STED imaging for colocalization analyses. *Opt. Express*. 19:3130–3143.
6. Donnert, G., J. Keller, ..., S. W. Hell. 2007. Two-color far-field fluorescence nanoscopy. *Biophys. J.* 92:L67–L69.
7. Auksoorius, E., B. R. Boruah, ..., P. M. W. French. 2008. Stimulated emission depletion microscopy with a supercontinuum source and fluorescence lifetime imaging. *Opt. Lett.* 33:113–115.
8. Moffitt, J. R., C. Osseforth, and J. Michaelis. 2011. Time-gating improves the spatial resolution of STED microscopy. *Opt. Express*. 19:4242–4254.
9. Dyba, M., and S. W. Hell. 2003. Photostability of a fluorescent marker under pulsed excited-state depletion through stimulated emission. *Appl. Opt.* 42:5123–5129.
10. Löscherberger, A., S. van de Linde, ..., M. Sauer. 2012. Super-resolution imaging visualizes the eightfold symmetry of gp210 proteins around the nuclear pore complex and resolves the central channel with nanometer resolution. *J. Cell Sci.* 125:570–575.
11. Honigmann, A., V. Mueller, ..., C. Eggeling. 2012. STED microscopy detects and quantifies liquid phase separation in lipid membranes using a new far-red emitting fluorescent phosphoglycerolipid analogue. *Faraday Discuss.* 161:77–89.
12. Hase, M. E., N. V. Kuznetsov, and V. C. Cordes. 2001. Amino acid substitutions of coiled-coil protein Tpr abrogate anchorage to the nuclear pore complex but not parallel, in-register homodimerization. *Mol. Biol. Cell*. 12:2433–2452.
13. Wurm, C. A., D. Neumann, ..., S. Jakobs. 2010. Sample preparation for STED microscopy. *Methods Mol. Biol.* 591:185–199.
14. Wurm, C. A., K. Kolmakov, ..., S. W. Hell. 2012. Novel red fluorophores with superior performance in STED microscopy. *Opt. Nano.* 1:1–7.
15. Cordes, V. C., A. Gajewski, ..., G. Krohne. 1995. Immunocytochemistry of annulate lamellae: potential cell biological markers for studies of cell differentiation and pathology. *Differentiation*. 58:307–312.
16. Schwille, P., F. J. Meyer-Almes, and R. Rigler. 1997. Dual-color fluorescence cross-correlation spectroscopy for multicomponent diffusional analysis in solution. *Biophys. J.* 72:1878–1886.
17. Mueller, V., C. Ringemann, ..., C. Eggeling. 2011. STED nanoscopy reveals molecular details of cholesterol- and cytoskeleton-modulated lipid interactions in living cells. *Biophys. J.* 101:1651–1660.